Experimental 25-Mb/s Wireless Infrared Link Using 4-PPM with Scalar Decision-Feedback Equalization

David C. Lee and Joseph M. Kahn

Department of Electrical Engineering and Computer Sciences
University of California, Berkeley, CA 94720

Abstract

We report a non-line-of-sight optical link for short-range, indoor data transmission at 25 Mb/s. The optical link uses a ceiling-directed beam and a wide-field-of-view receiver. The system uses 4-pulse-position modulation (4-PPM) with scalar decision-feedback equalization (SDFE), achieving low bit-error rates with a range of two meters in the presence of background light and multipath-induced intersymbol interference. We observe that the gain in electrical SNR efficiency from equalization is about 0.5 dB larger than theory, which we attribute to timing-offset errors in the unequalized system. We verify that the near-d.c. noise caused by electronic ballast-driven fluorescent lamps has a negligible impact on the system performance.

1. Introduction

Infrared (IR) radiation using intensity modulation with direct detection is a viable medium for short-range, indoor, wireless communication [1]-[3]. IR offers an enormous unregulated bandwidth and is free from interference between links operating in rooms separated by walls or other opaque barriers. Systems that use wide-beam transmitters and receivers with a wide field of view (FOV) provide ease of use. Non-line-of-sight links provide robustness against shadowing. While the spatial diversity of large-area, square-law photodetectors prevent multipath fading in such systems, multipath dispersion causes intersymbol interference (ISI) that can severely affect system performance above 10 Mbaud [3].

Pulse-position modulation (PPM) offers high average-power efficiency, but due to its poor bandwidth efficiency, it is more susceptible to multipath-induced ISI than simple on-off keying (OOK). In order to mitigate the effects of ISI, Barry [4] discussed various equalizers for PPM, including scalar decision-feedback equalization (SDFE). Audeh *et al.* [5] recently analyzed the performance of SDFE for PPM. We have modified an experimental IR system that used OOK with DFE [6] in order to implement a 4-PPM system with SDFE. In this paper we present results on the performance gain provided by SDFE for 4-PPM, comparing it to theory for a variety of channels and ambient-lighting conditions.

In particular, fluorescent lamps driven by electronic ballasts emit strong IR signals that are periodically intensity-modulated at kHz rates, containing spectral components up to about 1 MHz that can severely degrade the performance of IR links [6],[7]. Narasimhan *et al.* [7] have shown that OOK links can suffer penalties of several dB from fluorescent-light noise, making it necessary to reduce the interference using high-pass filtering. With non-return-to-zero transmitted pulses, this necessitates the use of line-coding [8] or quantized feedback [6] to prevent baseline wander. By contrast, PPM links operating above 10 Mb/s should, in theory, be largely unaffected by fluorescent-light noise, even without high-pass filtering [7]. Here, we verify this prediction.

2. System Description

The optical link, shown in Fig. 1, is a hybrid, non-line-of-sight (non-LOS) system [3] that uses a ceiling-directed transmitter and a wide-FOV receiver. The transmitter described in [6] was modified to produce eight steerable, collimated beams for use in multibeam transmission. However, for the purposes of this experiment, all eight beams were directed straight upwards to form one central spot on the ceiling, which produces a wide-beam, Lambertian pattern. The center wavelengths of the transmit beams vary from 805 nm to 808 nm with 10 dB-linewidths of 2.4 nm to 3.4 nm. When fully modulated by a 4-PPM signal, the transmitter emits a total optical average power of 300 mW.

The optical receiver described in [6] consists of a 1-cm^2 silicon *p-i-n* photodiode coupled to a high-index hemispherical concentrator, which in turn is covered by an optical bandpass filter with a center wavelength of 815 nm, a bandwidth of 30 nm, and a peak transmission of 68%. The lens-filter combination achieves a FOV of 65° (half-angle at half-effective area). The effective area of the combined lens, filter, and photodiode for illumination incident normal to the photodiode surface is 1.2 cm^2.

The receiver photocurrent is amplified by a 10-kΩ high-impedance preamplifier, followed by an equalizer to compensate for the single pole at 455 kHz formed by the load resistance and the 35-pF photodiode capacitance. Under a reverse bias of −180 V, the 3-dB bandwidth, which is limited by the transit time of the photodiode, is 25 MHz. A 30-MHz, five-pole, Bessel, low-pass filter bandlimits the shot noise and receiver thermal noise. The equivalent one-sided, input-referred noise current density is 6.4 pA/√Hz, averaged over the bandwidth of the Bessel filter.

A SDFE, consisting of analog tapped delay lines and manually controlled tap gains, reduces the multipath-induced ISI. The forward and reverse filters each consist of four taps with half-chip and unit-chip spacing, respectively. The filter taps are manually adjusted to minimize the BER. A slicer makes tentative chip decisions solely for the purpose of feedback equalization.

Finally, a soft-decision, PPM block decoder, consisting of an 8-bit, 125 Msample/s, SONY CXA1396D analog-to-digital converter (ADC) and discrete ECL logic for choosing the largest chip sample in each symbol, converts the PPM signal back into a bit stream. Eight bits provide sufficient quantization so that the

0-7803-4788-9/98/$10.00

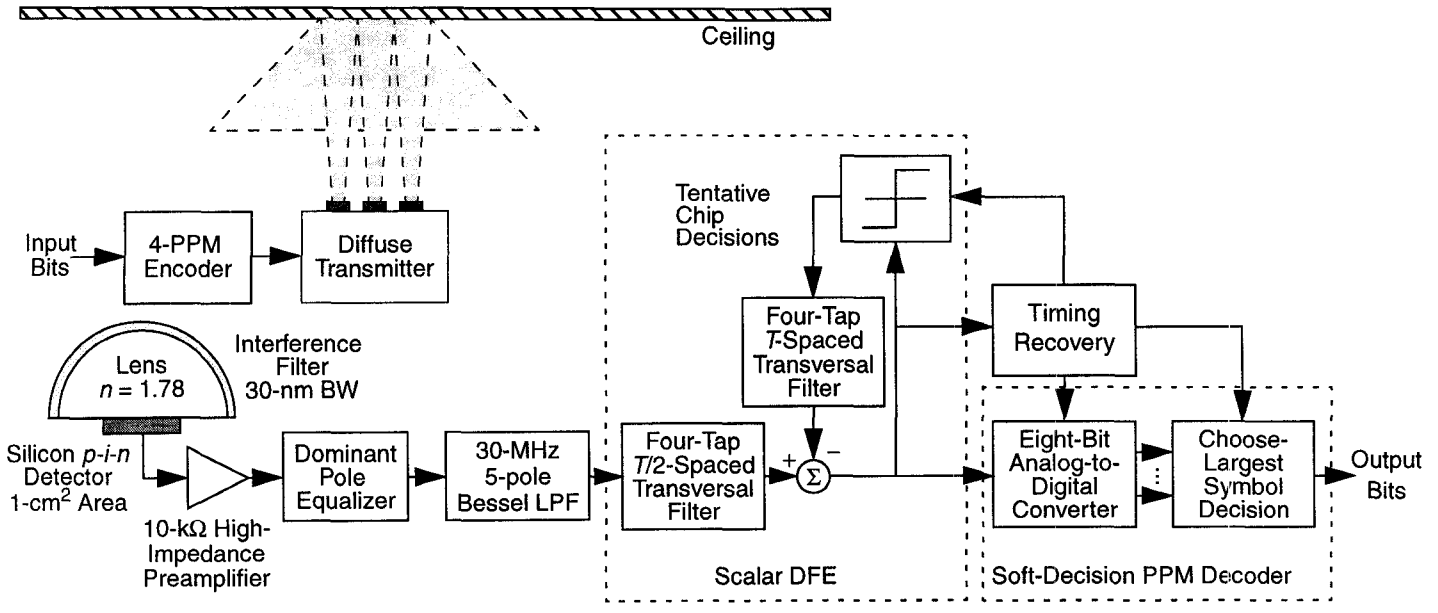

Fig. 1 System block diagram. The 806-nm transmitter emits a beam directed at the ceiling with an average output power of 300 mW when modulated by 4-PPM data. The receiver optics consist of a narrow-band, hemispherical optical filter bonded to the surface of a glass hemisphere. A 1-cm^2 silicon *p-i-n* photodiode drives a hybrid high-impedance amplifier followed by a 30-MHz low-pass filter. A scalar decision-feedback equalizer uses tentative chip decisions from the slicer to reduce the effect of multipath-induced intersymbol interference. A soft-decision PPM block decoder chooses the largest chip sample in each symbol and converts it into output bits.

ADC quantization noise is negligible in comparison to the shot noise and thermal noise. Phase-locked loops similar to those described in [9] and [10] provide chip- and symbol-clock recovery, respectively.

3. System Characterization

We characterized the system performance in two ways. First, we quantified the impact of multipath interference with and without SDFE. In these measurements, ambient lighting was weak, increasing the range of operation. This allowed us to take measurements on channels with delay spreads up to 9.0 ns. On channels with delay spreads beyond 9 ns, OOK with DFE is predicted to require less average optical power than 4-PPM with SDFE at 25 Mb/s [5]. Second, we measured the system performance under different lighting conditions in order to quantify the impact of ambient light noise.

3.1 Performance with Multipath Distortion

We measured the system performance in three different rooms: a hallway, a large conference room, and a small laboratory (Rooms A, C, and D in [6], respectively). All of the rooms had off-white-colored walls and ceilings. Within each room, we took measurements at four different transmission distances. These measurements consisted of an unequalized bit-error rate (BER) curve, an equalized BER curve, the link frequency response, and the average received optical power. The system used a 2,000-bit pseudo-random sequence (1,000 4-PPM symbols).

Each link frequency response consists of the combined response of the transmitter, multipath channel, photodetector, preamplifier, and dominant-pole equalizer. Inverse Fourier transformation of the frequency response combined with a Hamming window with a 100-MHz cutoff frequency yields the channel impulse response. The r.m.s. delay spread of the impulse response provides a useful measure of the impact of multipath ISI [11]. Fig. 2 shows how, for a given room, the delay spread increases from 6.7 ns to 9.0 ns as the transmission distance increases. Note that much of this delay spread is actually due to the transit-time-limited response of the photodiode. The delay

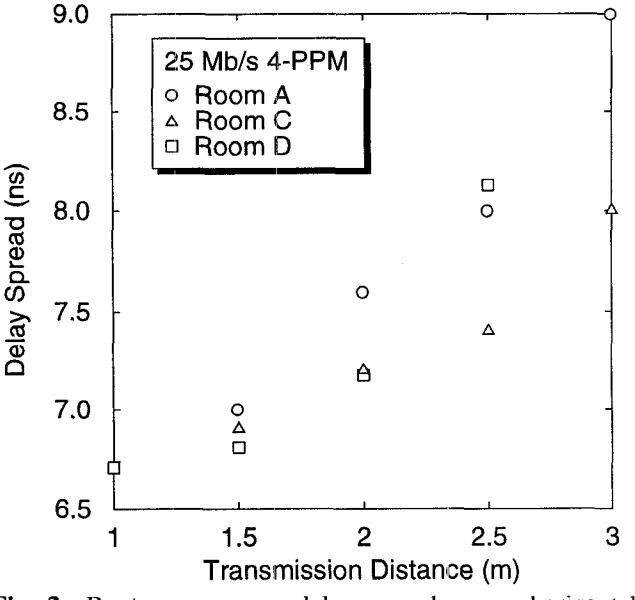

Fig. 2 Root-mean-square delay spread versus horizontal separation between transmitter and receiver. Note that the delay spread increases slightly as the transmission distance increases.

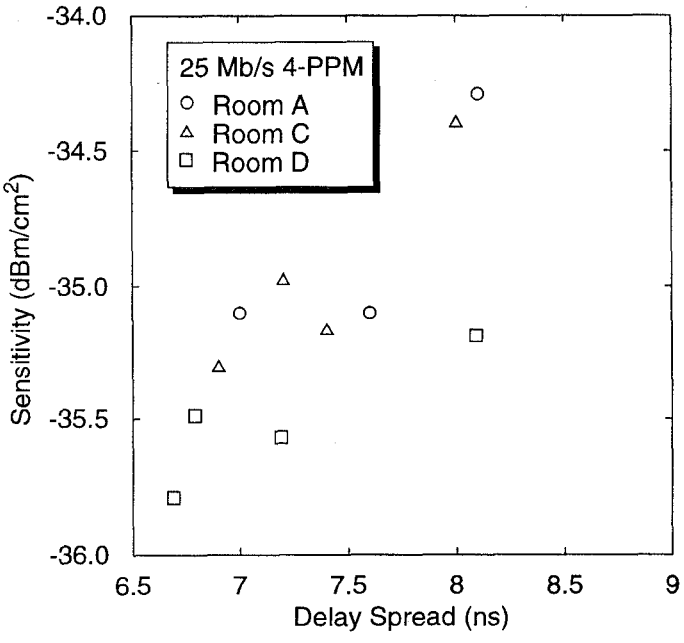

Fig. 3 Equalized receiver sensitivity at 10^{-4} BER versus root-mean-square delay spread. Note that the required illumination increases as the r.m.s. delay spread increases.

spread of the receiver alone (consisting of the photodiode, preamplifier, and dominant-pole equalizer) is 6.5 ns.

Fig. 3 displays the DFE receiver sensitivity versus r.m.s. delay spread, where the sensitivity is defined as the received irradiance at which the system achieves 10^{-4} BER. As the channel dispersion increases, more optical power is required to achieve the same BER.

The theoretical performance of the unequalized system is computed by averaging over all possible interfering symbol sequences of a length equal to the duration of the impulse response, which is truncated to finite duration if necessary, as detailed in [12] and summarized in the appendix. This computation assumes a receiver filter matched to the transmitted pulse shape, which results in uncorrelated noise samples in each chip, rather than the Bessel low-pass filter, which causes some correlation among noise samples in different chips. It provides an upper bound on the probability of bit error.

The theoretical performance of the SDFE system is computed for a receiver system that uses a filter matched to the convolution of the chip pulse shape with the channel impulse response, followed by a discrete-time noise whitener, followed by a zero-forcing (ZF) SDFE, as discussed in [5] and summarized in the appendix. This differs from the Bessel filter, and minimum-BER SDFE of the experimental system. Fortunately, the difference in performance between a ZF-DFE and minimum-BER DFE is small, particularly at low BER's, for pulse amplitude modulation [13]. The present work verifies this to be true for PPM, too. The theoretical analysis enumerates all possible incorrect chip decisions made by the slicer, and quantifies their effect, weighted by their probability of occurring. It provides an upper bound on the probability of bit error.

For each set of data, we chose a BER at which to compare the performance of the system. These BER's, which range from 10^{-2} to 10^{-6}, are generally close to the lowest BER obtainable for each unequalized BER curve (i.e., the BER obtained at the highest average optical power transmitted). We then compared the measured gain in SNR due to equalization with the theoretical gain, as shown in Fig. 4. The data points lie close to a line of unit slope, tending to have measured gains about 0.5 dB higher than theoretical gains. This is probably due to timing-offset errors in the unequalized BER curves, which lie about one-half dB above the corresponding theoretical unequalized curves. The ISI in the unequalized system causes the horizontal eye opening to be much smaller than in the SDFE system, resulting in the unequalized system having much greater sensitivity to any timing-offset errors at the ADC.

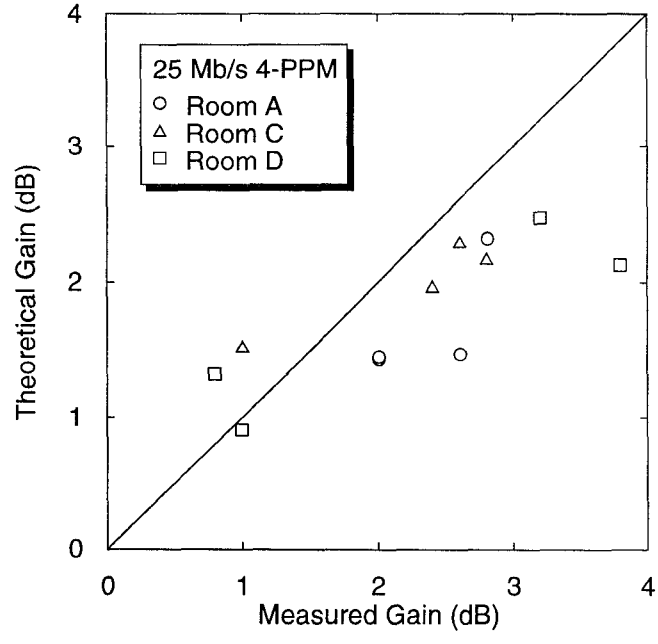

Fig. 4 Gain in electrical SNR efficiency due to scalar decision-feedback equalization at bit-error rates from 10^{-2} to 10^{-6}: comparison of theory and experiment. The data points lie close to a line of unit slope, with measured gains about 0.5 dB greater than theoretical gains.

3.2 Performance under Different Ambient-Lighting Conditions

Fluorescent lamps driven by electronic ballasts have a fundamental frequency at tens to hundreds of kHz, with significant harmonic components up to about 1 MHz [7]. For an OOK link, this interference can cause penalties of several dB, necessitating the use of high-pass filtering. With non-return-to-zero transmitted pulses, which have significant spectral components at and near d.c., line coding or quantized feedback is needed to compensate for resulting baseline wander [6],[7].

For an L-PPM link that uses soft-decision decoding, which chooses the largest of L chip samples in each symbol period,

however, it is not the value of the fluorescent-light waveform, but rather the change in value over the symbol period, that affects the decision device. This comparison over a block of L samples provides some immunity to the low-frequency, periodic interference, especially at high bit rates. Moreover, the PPM power spectral density goes to zero near d.c., so highpass filtering of PPM without line coding or active baseline restoration causes little penalty. Under typical office lighting conditions, we verify that at 25 Mb/s the symbol period is sufficiently short that the soft-decision 4-PPM block decoder, without high-pass filtering, is largely immune to the near-d.c., periodic noise caused by electronic ballast-driven, fluorescent lamps [7].

We measured the system performance in Room C under different lighting conditions at a transmission distance of 2.0 m. Fig. 5 shows the BER curves for the unequalized and SDFE systems with no light, with fluorescent light, and with bright skylight. The fluorescent lamps were driven by 22-kHz electronic ballasts, same as in [7]. The fluorescent light and skylight introduced receiver photocurrents of 57 μA and 178 μA, respectively. For the SDFE curves, fluorescent light and skylight result in electrical SNR penalties of 0.2 and 0.8 dB, respectively, at 10^{-6} BER. For the unequalized curves, the corresponding SNR penalties are 0.4 and 0.2 dB, respectively, at 10^{-5} BER. This shows that the penalty due to fluorescent lighting is due to the shot noise of the light, rather than the near-d.c. modulation caused by the electronic ballasts.

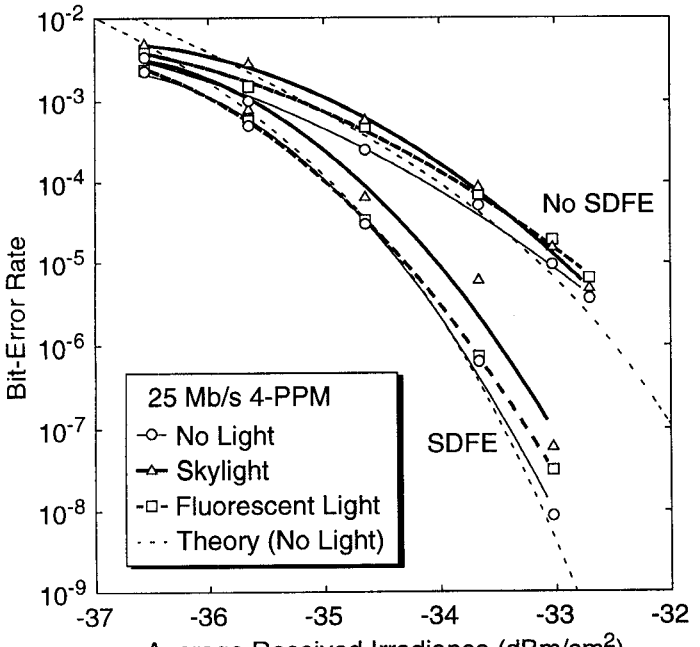

Fig. 5 Variation in performance of PPM system with and without scalar decision-feedback equalization due to ambient light. Data were taken in Room C, which has windows on two sides. Three different lighting conditions were used: no ambient light, fluorescent light, and bright skylight. Transmission distance was 2.0 m. For reference, theory curves for the case of no ambient light show excellent agreement with the corresponding measured curves.

4. Conclusions

We have demonstrated transmission of 25-Mb/s data at low BER using non-line-of-sight infrared radiation. 4-pulse position modulation (PPM) with scalar decision-feedback equalization (SDFE) is effective in mitigating the impact of multipath-induced ISI. We have shown that measured gains in electrical SNR efficiency due to SDFE, though about 0.5 dB larger than theoretical predictions due to timing-offset errors in the unequalized system, otherwise agree well with theory. At 25 Mb/s, soft-decision PPM decoding without high-pass filtering provides immunity to the low-frequency periodic intensity modulation of fluorescent-light noise caused by electronic ballasts.

5. Acknowledgments

The authors would like to thank J.T. Nee for wire-bonding the receiver, M.D. Audeh for assistance in calculating the theoretical performance of PPM with SDFE, and J.B. Carruthers and G.W. Marsh for helpful discussions about the optical link.

This research was supported by National Science Foundation Grant ECS-9710065, Hewlett-Packard Company, the University of California MICRO Program, and a Natural Sciences and Engineering Research Council of Canada Scholarship.

Appendix: Theoretical BER Analysis

The discrete-equivalent vector channel model for L-PPM is given by [4]:

$$\boldsymbol{y}_k = \boldsymbol{H}_k \otimes \boldsymbol{x}_k + \boldsymbol{n}_k = \boldsymbol{s}_k + \boldsymbol{n}_k \tag{1}$$

where $\boldsymbol{y}_k$, $\boldsymbol{x}_k$, $\boldsymbol{s}_k$, and $\boldsymbol{n}_k$ are length-L vectors representing the output, input, signal component, and noise, respectively, sampled at the chip rate $(L/\log_2 L)R_b$, where $R_b = 25$ Mb/s is the bit rate. The channel impulse response is a Toeplitz sequence $[\boldsymbol{H}_k]_{ij} = h_{kL+i-j}$, where h_j is the discrete-equivalent impulse response representing the combination of transmitter filter, multipath channel, and receiver filter. The channel length K in symbols is the index of the last nonzero term in $\boldsymbol{H}_k$. For unequalized PPM, the receiver filter is matched to the transmitter pulse shape. For PPM with SDFE, the receiver filter is a whitened-matched filter. Let P be the received optical power, R the photodiode responsivity, and N_0 the noise power spectral density (PSD). We normalize h_j according to $\sum h_j = LPR/\sqrt{N_0}$, the peak received photocurrent divided by the square root of the noise PSD. The noise samples $\boldsymbol{n}_k$ are white and Gaussian with zero mean and unit variance.

For unequalized PPM, the output vectors $\boldsymbol{y}_k$ are sent to a soft-decision PPM block decoder, which makes symbol decisions $\hat{\boldsymbol{x}}_k$ based on the largest sample among each length-L vector, producing the estimated information bits.

Symbol $i \in \{0, \ldots, L-1\}$ results in a length-L vector of chips, or codeword denoted $\boldsymbol{c}_i$, with a one in position i, and zero elsewhere. Let $C \in \{\boldsymbol{c}_0, \ldots, \boldsymbol{c}_{L-1}\}$ denote the set of L codewords. Given a transmitted codeword $\boldsymbol{x}_k = \boldsymbol{c}_i$, and previously transmitted codewords $\boldsymbol{X} = \{\ldots, \boldsymbol{x}_{k-2}, \boldsymbol{x}_{k-1}\}$, then for unequalized PPM, the probability of symbol error $\hat{\boldsymbol{x}}_k \neq \boldsymbol{x}_k$ is well-approximated at high SNR by the following union bound [12]:

$$P[\hat{x}_k \neq x_k | x_k = c_i, X] \leq \sum_{j=0, j\neq i}^{L-1} Q\left((c_i - c_j)^T \frac{s_k}{\sqrt{2}}\right) \quad (2)$$

Averaging over all possible codeword sequences and converting from symbol errors to bit errors gives:

$$P[\text{bit error}] \leq \frac{1}{L^{K+1}} \sum_{X \in C^K} \sum_{i=0}^{L-1} \sum_{j=0, j\neq i}^{L-1} m_{ij} Q\left((c_i - c_j)^T \frac{s_k}{\sqrt{2}}\right), \quad (3)$$

where m_{ij} is the number of information bits that differ between symbol i and j.

For SDFE, we view the channel model in scalar form given by:

$$y_j = h_j \otimes x_j + n_j, \quad (4)$$

where $y_k = (y_{kL}, \ldots, y_{kL+L-1})^T$, and similarly for the input and noise vectors.

A chip-rate slicer makes tentative decisions $\hat{x}_j$ on the filtered signal y_j, which is fed into a feedback filter that cancels the intra-symbol as well as intersymbol interference using the ZF criterion. The slicer threshold is set to the minimax value of $\lambda = h_0/2$, since we assume independent chip decisions. If h_j is monotonically decreasing, then this will maximize π_0, the probability that all chips in a symbol are detected correctly. The feedback filter has an impulse response $h_j - h_0\delta_j$. The equalized signal is given by:

$$r_j = y_j - \hat{x}_j \otimes (h_j - h_0\delta_j). \quad (5)$$

These samples are grouped into length-L vectors r_k and sent to the same "choose-largest" PPM block decoder as for unequalized PPM.

Let Y denote the event that all previous chip decisions from prior PPM codewords are correct, a standard assumption in DFE analyses [13]. The analysis of the performance of PPM with SDFE involves enumerating all possible chip-decision errors that the slicer makes, quantifying their effects, and weighing the conditional error probabilities by their respective probabilities of occurring. Table 1 summarizes the various probability terms and their descriptions. The probability of symbol error given that Y is true is bounded from above by:

$$P[\text{err}|\text{Y}] \leq \frac{1}{L} \sum_{l=0}^{L-1} \left\{ \sum_{j=0}^{l-1} P_{1,j}\pi_{1,j} + P_2\pi_2 + \sum_{j=l+1}^{L-1} P_{3,j}\pi_{3,j} + P_4\pi_4 \right\} \quad (6)$$

Due to space constraints, we are unable to reprint the exact expressions for these probability terms. Please refer to [5] for a derivation and a more detailed explanation.

To convert from symbol-error to bit-error probability, we multiply (6) by the factor $(L/2)/(L-1)$, which represents an average number of bit errors per symbol error [8]. Strictly speaking, this factor is only valid for unequalized PPM on the ideal channel, but in practice it is fairly accurate for this application, too [5].

Table 1: Probability terms for bound on performance of SDFE of PPM.

Symbol	Description
$P_{1,j}$	Prob. error given false alarm at j before tx chip at l
$\pi_{1,j}$	Prob. of false alarm at j before tx chip at l
P_2	Prob. error given missed chip at l
π_2	Prob. of missed chip at l
$P_{3,j}$	Prob. error given false alarm at j after tx chip at l
$\pi_{3,j}$	Prob. of false alarm at j after tx chip at l
P_4	Upper bound on prob. error given two or more chip-decision errors
π_4	Prob. of two or more chip-decision errors

References

1. F. R. Gfeller and U. H. Bapst, "Wireless In-House Data Communication via Diffuse Infrared Radiation," *Proc. of the IEEE*, vol. 67, no. 11, pp. 1474-1486, Nov. 1979.
2. J.R. Barry, *Wireless Infrared Communications*, Kluwer Academic Publishers, Boston, 1994.
3. J.M. Kahn and J.R. Barry, "Wireless Infrared Communications," *Proc. of the IEEE*, vol. 85, no. 2, pp. 265-98, Feb. 1997.
4. J.R. Barry, "Sequence Detection and Equalization for Pulse-Position Modulation", in *Proc. of IEEE Intl. Conf. on Commun. (ICC '94)*, New Orleans, LA, May 1-5, 1994, pp. 1561-1565.
5. M.D. Audeh, J.M. Kahn, and J.R. Barry, "Decision-Feedback Equalization of Pulse-Position Modulation on Measured Indoor Infrared Channels," in *Proc. of IEEE Intl. Conf. on Commun. (ICC '96)*, vol. 2, pp. 1220-6, Dallas, TX, June 23-27, 1996.
6. G.W. Marsh and J.M. Kahn, "Performance Evaluation of Experimental 50-Mb/s Diffuse Infrared Wireless Link Using On-Off Keying with Decision-Feedback Equalization," *IEEE Trans. Commun.*, vol. COM-44, pp. 1496-1504, Nov. 1996.
7. R. Narasimhan, M.D. Audeh, and J.M. Kahn, "Effect of Electronic-Ballast Fluorescent Lighting on Wireless Infrared Links," *IEE Proc. - Optoelectronics*, vol. 143, no. 6, pp. 347-354, Dec. 1996.
8. M.D. Audeh and J.M. Kahn, "Performance Evaluation of Baseband OOK for Wireless Indoor Infrared LAN's Operating at 100 Mb/s," *IEEE Trans. Commun.*, vol. COM-43, pp. 2085-2094, June 1995.
9. F. Davidson and X. Sun, "Slot Clock Recovery in Optical PPM Communication Systems with Avalanche Photodiode Photodetectors," *IEEE Trans. Commun.*, vol. COM-37, pp. 1164-1171, Nov. 1989.
10. X. Sun and F. Davidson, "Word Timing Recovery in Direct Detection Optical PPM Communication Systems with Avalanche Photodiodes Using A Phase Lock Loop," *IEEE Trans. Commun.*, vol. COM-38, pp. 666-673, May 1990.
11. J.M. Kahn, W.J. Krause, and J.B. Carruthers, "Experimental Characterization of Non-Directed Indoor Infrared Channels," *IEEE Trans. Commun.*, vol. COM-43, pp. 1613-1623, Feb.-April 1995.
12. M.D. Audeh and J.M. Kahn, "Performance of Pulse-Position Modulation on Measured Non-Directed Indoor Infrared Channels," *IEEE Trans. Commun.*, vol. COM-44, pp. 654-659, June 1996.
13. C.A. Belfiore and J.H. Park, Jr., "Decision Feedback Equalization," *Proc. of the IEEE*, vol. 67, no. 8, pp. 1143-1156, Aug. 1979.